J. Fluid Mech. (1983), *vol.* 126, *pp.* 431–442
Printed in Great Britain

A new type of boundary layer in a rapidly rotating gas

By TAKUYA MATSUDA AND KEIZO NAKAGAWA
Department of Aeronautical Engineering, Kyoto University, Japan

(Received 26 April 1982)

Gaseous flow in a pie-shaped cylinder of infinite length rotating about the apex is considered. The horizontal flow is induced either by the temperature distribution or by the source/sink distribution on the walls θ = constant. It is found that along the vertical walls θ = constant the $E^{\frac{1}{2}}$ boundary layer is formed, where E is the Ekman number. Although the equation governing the above boundary layer is very similar to that of the Ekman layer, it is a new type of boundary layer which may be called the buoyancy layer. Along the wall on which r is constant thermal boundary layers very similar to the Stewartson layers are found to be formed. The role of these layers is to mediate the temperature jump. These layers disappear in the incompressible limit.

1. Introduction and summary

The dynamics of a rotating gas has been developed for the gas centrifuge (Sakurai & Matsuda 1974; Nakayama & Usui 1974; for complete references see Rätz 1978; Soubbaramayer 1979). Since researchers were interested in the flow in a rotating circular cylinder, they assumed an axisymmetry, except in the work of Matsuda, Sakurai & Takeda (1975), who studied the effect of the non-axisymmetric distribution of the source/sink in a circular cylinder. On the other hand Kuo & Veronis (1971) studied an incompressible flow induced by a source/sink in a pie-shaped rotating basin with a free surface. They found that the ϵ-layer is formed along the western boundary (θ = constant) and the $\epsilon^{\frac{1}{2}}$ layer along the r = constant wall, where $\epsilon = E^{\frac{1}{2}}/F$ and F is the Froude number. It would be interesting to see the compressible couterpart of the Kuo–Veronis flow. Matsuda, Nakagawa & Takeda (1981) considered a non-axisymmetric compressible flow, although they restricted themselves to a circular cylinder with inclined bottom surface. It was found that the bottom topography has a minor effect on the flow.

In the present paper we consider a compressible flow in a pie-shaped cylinder. In order to avoid undue complexity, we assume the cylinder to be infinitely long and all flow variables to be independent of the axial coordinate z. The cylinder rotates about the apex $r = 0$ so rapidly that the radial-pressure scale height is comparable to the cylinder radius L (see figure 1). Since we wish to compare the flow field in the pie-shaped cylinder with that in an axisymmetric circular cylinder with end plates, both cases will be dealt with together.

Before a detailed discussion is given using the full equations, let us summarize the present result. Figure 2 shows the (r, z) cross-section of the circular cylinder and the (r, θ) cross-section of the pie-shaped cylinder. The compressible flow in a rapidly rotating circular cylinder has been investigated by many workers (see references cited above) and is well understood.

Along the top and the bottom cover of the axisymmetric cylinder, the Ekman layer

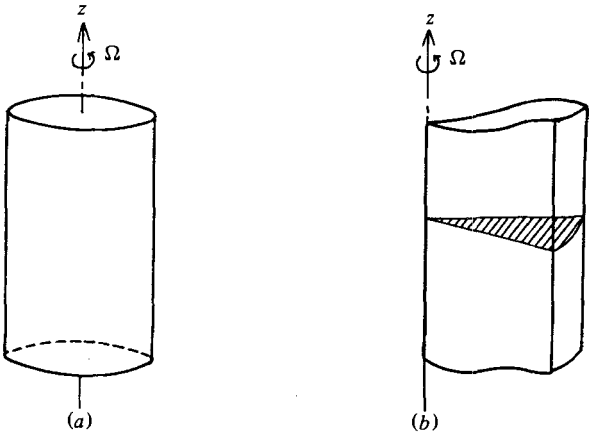

FIGURE 1. (*a*) Schematic representation of a rapidly rotating circular cylinder. (*b*) Infinitely long pie-shaped cylinder rotating about the apex.

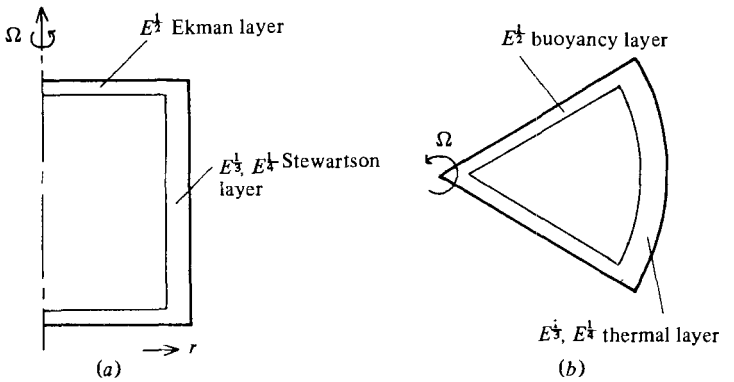

FIGURE 2. (*a*) The (r, z) cross-section of the circular cylinder. Along the top and the bottom cover the $E^{\frac{1}{2}}$ Ekman layers are formed, while the $E^{\frac{1}{3}}$ and $E^{\frac{1}{4}}$ Stewartson layers are generated along the sidewall. The rest is the inner core. (*b*) The (r, θ) cross-section of the pie-shaped cylinder. Along the walls θ = constant the $E^{\frac{1}{2}}$ buoyancy layers are formed. Along the outer wall the $E^{\frac{1}{3}}$ and $E^{\frac{1}{4}}$ thermal layers are produced. The rest is the inner core.

with thickness $E^{\frac{1}{2}}$ is formed, while the Stewartson $E^{\frac{1}{3}}$ and $E^{\frac{1}{4}}$ layers are formed along the sidewall (see figure 2*a*). In the pie-shaped cylinder three kinds of boundary layer are found (see figure 2*b*). Along the wall θ = constant a boundary layer with thickness $E^{\frac{1}{2}}$ is formed. Let us call this layer a buoyancy layer. The equation governing the layer is

$$\frac{\partial^4 \hat{u}}{\partial \eta^4} + 4hr^6 \epsilon_{\mathrm{R}}^2 \hat{u} = 0, \tag{1.1}$$

where quantities with a hat represent the boundary-layer values, η is the stretched azimuthal coordinate, h a compressibility parameter and ϵ_{R} the normalized density (see §2 for details). Here we use a cylindrical coordinate system rotating with the

cylinder, and (u, v, w) are the velocity components in the (r, θ, z)-directions. Equation (1.1) is essentially the same as the governing equation for the Ekman layer:

$$\frac{\partial^4 \hat{u}}{\partial \eta'^4} + 4(l + hr^2)\,\epsilon_R^2\,\hat{u} = 0, \tag{1.2}$$

where η' is a stretched coordinate of z. Note that the buoyancy layer disappears in the limit $h \to 0$, while the Ekman layer remains. A buoyancy layer on a vertical wall in an axially stratified Boussinesq fluid was discussed by Barcilon & Pedlosky (1967). Our buoyancy layer is a compressible counterpart of their layer.

On the outer wall $r = L$, a thermal boundary layer with thickness $E^{\frac{1}{3}}$ is formed. The governing equation for it is

$$\frac{\partial^6 \overline{T}}{\partial \zeta^6} + 4h\frac{\partial^2 \overline{T}}{\partial \theta^2} = 0, \tag{1.3}$$

where quantities with a bar denote the boundary-layer variables, and ζ a radial stretched coordinate. Equation (1.3) is also very similar to the equation for the Stewartson $E^{\frac{1}{3}}$ layer as

$$\frac{\partial^6 \overline{T}}{\partial \zeta^6} + 4(1 + h)\frac{\partial^2 \overline{T}}{\partial z^2} = 0, \tag{1.4}$$

if θ is replaced by z. A close similarity between (1.3) and (1.4) is obvious. It should be noticed that the $E^{\frac{1}{3}}$ thermal layer disappears in the incompressible limit, i.e. $h \to 0$, while the Stewartson layer still exists. In the inner core, all quantities are functions only of r. Therefore the role of the above thermal layer is to mediate the discrepancy of the inner temperature $T_i(r = L)$ and the wall temperature $T_{w2}(\theta)$.

These two equations (1.3) and (1.4) are actually not independent. In fact they are two limiting cases of a unified equation:

$$\frac{\partial^6 \overline{T}}{\partial \zeta^6} + 4(1 + h)\frac{\partial^2 \overline{T}}{\partial z^2} + 4h\frac{\partial^2 \overline{T}}{\partial \theta^2} = 0. \tag{1.5}$$

A boundary layer described by (1.5) may be called a generalized Stewartson $E^{\frac{1}{3}}$ layer, which is a combination of a conventional Stewartson layer and our thermal layer.

Figure 3 illustrates the antisymmetric flows for both the circular cylinder and the pie-shaped cylinder. In the case of the circular cylinder the top cover rotates slightly more slowly than the bottom. The gas in the inner core rotates with the mean angular velocity of the top and the bottom cover, i.e. $v_i = \frac{1}{2}(v_T + v_B)$. In order to match a no-slip condition at the top and the bottom, the Ekman layers are formed. In the Ekman layers $(\hat{u}, \hat{v})$ form what is called an Ekman spiral, whose driving force is the Coriolis force. Through the continuity equation the axial velocity component $\hat{w}$ of order $E^{\frac{1}{2}}$ is induced. It approaches the axial velocity w_i in the inner core at the outer boundary of the Ekman layer. This mechanism is called the Ekman pumping. Since u_i is of order E in the inner core, the fluid pumped at the top Ekman layer flows axially and is sucked in at the bottom Ekman layer. This fluid is recirculated to the top through the sidewall Stewartson layer.

A similar antisymmetric flow pattern is realized when the temperature of the top cover is kept slightly higher than the bottom while they rotate with the same angular speed. This is called a thermally driven flow, while the above case is called a mechanically driven one. In the inner core an azimuthal flow called a thermal wind is established. The azimuthal velocity v_i of the thermal wind is a function of z. In

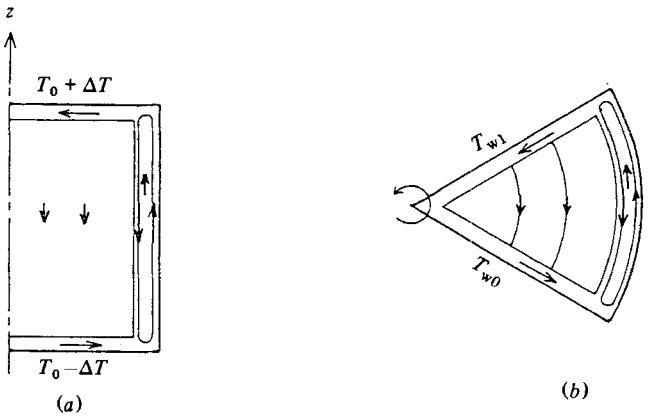

FIGURE 3. (*a*) Schematic representation of a mechanically/thermally driven antisymmetric flow in the rotating cylinder. A vertical flow of order $E^{\frac{1}{2}}$ is generated in the inner core by the Ekman pumping mechanism. This flow recirculates through the $E^{\frac{1}{3}}$ Stewartson layer. A closed circulation of order $E^{\frac{1}{3}}$ is induced in the Stewartson layer for a thermally driven case. (*b*) Schematic representation of a thermally driven antisymmetric flow in the rotating pie-shaped cylinder. An azimuthal flow of order $E^{\frac{1}{2}}$ is induced in the inner core by the buoyancy pumping mechanism.

order to satisfy the no-slip condition at the sidewall $r = L$, a closed circulation is induced in the Stewartson layer, as is shown in figure 3(*a*).

Now let us consider a pie-shaped cylinder. As is shown in figure 3(*b*), the temperature T_{w1} of the wall $\theta = \theta_1$ is kept slightly higher than T_{w0} of the wall $\theta = 0$. In the inner core, the temperature T_i depends on r only. It turns out that $T_i = \frac{1}{2}(T_{w0} + T_{w1})$. Therefore there must be thermal layers at the walls. In the boundary layer at $\theta = \theta_1$ a centripetal flow is induced by a buoyancy force, while a centrifugal flow is established in the layer at $\theta = 0$. The driving force of these flows is a buoyancy force, and therefore these boundary layers can be called the buoyancy layers.

In the buoyancy layer $(\hat{u}, \hat{T})$ play a similar role to $(\hat{u}, \hat{v})$ in the Ekman layer, and $\hat{v}$ plays the role of $\hat{w}$. An inner flow v_i of order $E^{\frac{1}{2}}$ is excited by the buoyancy pumping mechanism. The inner flow recirculates through the sidewall thermal layer.

If the sidewall $r = L$ has a temperature distribution, a closed circulation is produced in order to match the temperature; this situation is shown in figure 3(*b*). These situations are very similar to the circular-cylinder case.

Figure 4 shows the symmetric flow, which is sometimes called the externally driven flow or the source–sink flow. The analysis of the symmetric flow in the circular cylinder was given by Matsuda *et al.* (1975). Let us summarize the results. If one assumes the source/sink distribution at the top and the bottom cover to be w_T and w_B, the axial flow $w_i = \frac{1}{2}(w_T + w_B)$ is established in the inner core. An azimuthal flow v_i is also excited by the radial pressure gradient, and is called a geostrophic wind. A horizontal transport of the fluid occurs only through the top and the bottom Ekman layers, as shown in figure 4(*a*).

In the case of the pie-shaped cylinder let us assume a source/sink distribution v_{w0} and v_{w1} at the walls $\theta = 0$ and $\theta = \theta_1$. The source/sink flow velocities are assumed to be of order $E^{\frac{1}{2}}$. In the inner core an azimuthal flow $v_i = \frac{1}{2}(v_{w0} + v_{w1})$ of order $E^{\frac{1}{2}}$ is established, and the horizontal transport occurs through the $E^{\frac{1}{2}}$ buoyancy layers. In the present case there is no flow corresponding to the geostrophic wind, although an excess temperature is induced in the inner core.

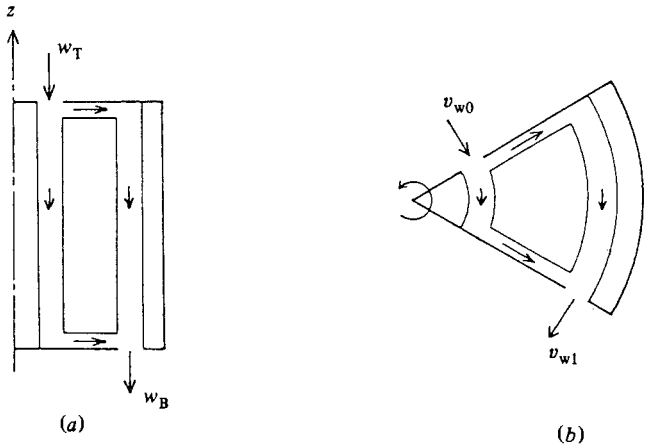

FIGURE 4. (*a*) Schematic representation of an externally driven symmetric (source/sink flow) in the circular cylinder. (*b*) Same as (*a*) except for the pie-shaped cylinder.

Although we will not discuss it in detail, it is clear that the $E^{\frac{1}{4}}$ Stewartson layer in the circular cylinder has its counterpart, namely the $E^{\frac{1}{4}}$ thermal layer, in the pie-shaped cylinder.

The close similarity between the flows in the circular cylinder and the pie-shaped cylinder has been discussed so far. Nevertheless there is a difference. As can be easily seen from (1.1)–(1.4), the buoyancy layer and the thermal layer in the pie-shaped cylinder disappear in the limit $h \to 0$, i.e. the incompressible limit. On the other hand the Ekman layer and the Stewartson layer exist for both incompressible and compressible fluid.

2. Basic equations

The linearized non-dimensional equations describing a steady motion of rapidly rotating gas are written in the rotating frame as

$$\operatorname{div}\mathbf{q} + G_0 ru = 0, \tag{2.1}$$

$$-2v + rT + \frac{1}{G_0}\frac{\partial P}{\partial r} = \frac{E}{\epsilon_R}\left[Lu + \frac{1}{3}\frac{\partial}{\partial r}(\operatorname{div}\mathbf{q}) - \frac{2}{r^2}\frac{\partial v}{\partial \theta}\right], \tag{2.2}$$

$$2u + \frac{1}{G_0 r}\frac{\partial P}{\partial \theta} = \frac{E}{\epsilon_R}\left[Lv + \frac{1}{3r}\frac{\partial}{\partial \theta}(\operatorname{div}\mathbf{q}) + \frac{2}{r^2}\frac{\partial u}{\partial \theta}\right], \tag{2.3}$$

$$\frac{1}{G_0}\frac{\partial P}{\partial z} = \frac{E}{\epsilon_R}\left[\Delta w + \frac{1}{3}\frac{\partial}{\partial z}(\operatorname{div}\mathbf{q})\right], \tag{2.4}$$

$$-4hru = \frac{E}{\epsilon_R}\Delta T, \tag{2.5}$$

$$P = \rho + T, \tag{2.6}$$

where

$$\operatorname{div}\mathbf{q} = \frac{1}{r}\frac{\partial}{\partial r}(ru) + \frac{1}{r}\frac{\partial v}{\partial \theta} + \frac{\partial w}{\partial z}, \quad \mathbf{q} = (u, v, w), \tag{2.7}$$

$$\Delta = \frac{1}{r}\frac{\partial}{\partial r}\left(r\frac{\partial}{\partial r}\right)+\frac{1}{r^2}\frac{\partial^2}{\partial\theta^2}+\frac{\partial^2}{\partial z^2}, \quad L = \Delta-\frac{1}{r^2}, \tag{2.8}$$

$$G_0 = \frac{ML^2\Omega^2}{RT_0}, \quad E = \frac{\nu}{\Omega L^2}, \quad h = \frac{(\gamma-1)\,Pr\,G_0}{4\gamma}, \tag{2.9}$$

$$\epsilon_R = \exp\{\tfrac{1}{2}G_0(r^2-1)\}. \tag{2.10}$$

Axisymmetric versions of (2.1)–(2.10) are given in Matsuda & Takeda (1978), in which G_0 in their equation (2.4) should be taken away. Non-axisymmetric parts were discussed in Matsuda *et al.* (1975). The length is normalized by the cylinder radius L, and the speed by the peripheral speed $L\Omega$, where Ω is an angular speed of the cylinder. Other quantities M, R, T_0, ν, γ and Pr are the molecular weight of the gas, the gas constant, the mean temperature, the kinematic viscosity, the ratio of specific heats, and the Prandtl number respectively. A parameter G_0 characterizing the system is nearly the square of rotational Mach number, and is assumed to be of the order of unity. The Ekman number E is assumed to be sufficiently small that a boundary-layer approximation is valid. The compressibility parameter h is of the order of unity.

The pie-shaped cylinder is restricted by three walls: $\theta = 0$, $\theta = \theta_1$ and $r = 1$. The boundary conditions applied on these three walls are

$$u = w = 0, \quad v = v_{w0}(r), \quad T = T_{w0}(r) \quad (\theta = 0), \tag{2.11}$$

$$u = w = 0, \quad v = v_{w1}(r), \quad T = T_{w1}(r) \quad (\theta = \theta_1), \tag{2.12}$$

$$u = v = w = 0, \quad T = T_{w2}(\theta) \quad (r = 1). \tag{2.13}$$

v_{w0} and v_{w1} are assumed to be of order $E^{\frac{1}{2}}$ in order to make the problem tractable.

3. Inner core

Far from the walls the effect of viscosity can be neglected, and such a region is called the inner core. The quantities in the inner core are denoted by the suffix i. Inspection of (2.5) leads to the conclusion that u is of order E in the inner core. As was discussed in §1, the order of magnitude of v is $E^{\frac{1}{2}}$ in the present treatment. Therefore quantities in the inner core can be scaled as follows:

$$u = Eu_i, \quad v = E^{\frac{1}{2}}v_i, \quad P = P_i, \quad T = T_i, \quad \rho = \rho_i. \tag{3.1}$$

Neglecting z-dependence, (2.1)–(2.6) reduce to

$$\frac{1}{r}\frac{\partial v_i}{\partial\theta} = 0, \tag{3.2}$$

$$rT_i+\frac{1}{G_0}\frac{\partial P_i}{\partial r} = 0, \tag{3.3}$$

$$\frac{1}{G_0 r}\frac{\partial P_i}{\partial\theta} = 0, \tag{3.4}$$

$$-4hru_i = \frac{1}{\epsilon_R}\Delta T_i, \tag{3.5}$$

$$P_i = \rho_i+T_i. \tag{3.6}$$

From (3.2)–(3.6) we conclude that all physical variables in the inner core are functions only of r as far as the lowest order is concerned. The density perturbation ρ_i does not play a primary role and will not be discussed further.

It is interesting to compare the present conclusion with that in Matsuda *et al.* (1975), who considered non-axisymmetric flow in a circular cylinder with θ-dependent boundary conditions on end covers. They concluded that the flow in the Ekman layer should not have θ-dependence. The θ-dependence of the boundary conditions on the end covers was mediated through a viscous effect in the inner core. In the present problem, on the other hand, the θ-dependence is applied on vertical walls. The flow in the inner core does not have θ-dependence because it is mediated through boundary layers. Therefore the effect of viscosity in the inner core can be neglected. If we neglect θ-dependence in the work by Matsuda *et al.* (1975) we reach the same conclusion as in the present paper.

4. The $E^{\frac{1}{2}}$ buoyancy layer

Let us consider the $E^{\frac{1}{2}}$ layer along the wall $\theta = 0$. Requiring the radial velocity to be of order unity, the inspection of the energy equation (2.5) leads to the conclusion that the thickness of the buoyancy layer is of order $E^{\frac{1}{2}}$. Then let us scale the boundary-layer quantities as follows:

$$u = \hat{u}, \quad v = E^{\frac{1}{2}}\hat{v}, \quad T = \hat{T}, \quad P = \hat{P}, \quad \theta = E^{\frac{1}{2}}\eta. \tag{4.1}$$

The substitution of (4.1) into (2.1)–(2.5) leads to

$$\frac{1}{r}\frac{\partial}{\partial r}(r\hat{u}) + \frac{1}{r}\frac{\partial \hat{v}}{\partial \eta} + G_0 r\hat{u} = 0, \tag{4.2}$$

$$r\hat{T} + \frac{1}{G_0}\frac{\partial \hat{P}}{\partial r} = \frac{1}{\epsilon_R r^2}\frac{\partial^2 \hat{u}}{\partial \eta^2}, \tag{4.3}$$

$$\frac{\partial \hat{P}}{\partial \eta} = 0, \tag{4.4}$$

$$-4hr\hat{u} = \frac{1}{\epsilon_R r^2}\frac{\partial^2 \hat{T}}{\partial \eta^2}. \tag{4.5}$$

From (4.4) we see that $\hat{P}$ depends only on r. Demanding that 'hatted' quantities approach the respective physical quantities in the inner core, we conclude that

$$\frac{\partial \hat{P}}{\partial r} = \frac{\partial P_i}{\partial r}. \tag{4.6}$$

Differentiating (4.3) with respect to η twice, and substituting (4.5) into the result, we obtain

$$\frac{\partial^4 \hat{u}}{\partial \eta^4} + 4hr^6\epsilon_R^2\hat{u} = 0. \tag{4.7}$$

The solution of (4.7) decaying at $\eta \to \infty$ is

$$\hat{u} = A_1 e^{(-1-i)\sigma\eta} + A_2 e^{(-1+i)\sigma\eta}, \tag{4.8}$$

where $\sigma = h^{\frac{1}{4}}r^{\frac{3}{2}}\epsilon_R^{\frac{1}{2}}$, and A_1 and A_2 are unknown functions of r to be determined later. From the boundary condition $\hat{u} = 0$ at $\eta = 0$ we can rewrite (4.8) as

$$\hat{u} = A_1(r)\,[e^{(-1-i)\sigma\eta} - e^{(-1+i)\sigma\eta}]. \tag{4.9}$$

Substituting (4.9) into (4.3), we have an expression for $\hat{T}$ as

$$\hat{T} = 2ih^{\frac{1}{2}} A_1[e^{(-1-i)\sigma\eta} + e^{(-1+i)\sigma\eta}] - \frac{1}{G_0 r}\frac{\partial P_i}{\partial r}. \tag{4.10}$$

The thermal boundary conditions are $\hat{T} = T_{w0}$ at $\eta = 0$ and $\hat{T} = T_i$ at $\eta \to \infty$. Using these conditions we have

$$4ih^{\frac{1}{2}} A_1 - \frac{1}{G_0 r}\frac{\partial P_i}{\partial r} = T_{w0}(r), \tag{4.11}$$

$$-\frac{1}{G_0 r}\frac{\partial P_i}{\partial r} = T_i. \tag{4.12}$$

Eliminating A_1 and $\hat{P}_i$ from (4.10), we obtain

$$\hat{T} = \tfrac{1}{2}(T_{w0} - T_i)[e^{(-1-i)\sigma\eta} + e^{(-1+i)\sigma\eta}] + T_i. \tag{4.13}$$

Now we have expressions for $\hat{u}$ and $\hat{T}$. By integrating (4.2) with respect to η, we can decide $\hat{v}$. After lengthy calculations we have

$$\hat{v} = -\frac{1}{2\sigma}\left[(1+G_0 r^2)A_1 + r\frac{\partial A_1}{\partial r}\right][(-1+i)e^{(-1-i)\sigma\eta} - (-1-i)e^{(-1+i)\sigma\eta}]$$
$$-\tfrac{1}{2}A_1(3+G_0 r^2)\left[\left(\eta - \frac{-1+i}{2\sigma}\right)e^{(-1-i)\sigma\eta} - \left(\eta - \frac{-1-i}{2\sigma}\right)e^{(-1+i)\sigma\eta}\right] + v_i(r), \tag{4.14}$$

where the condition $\hat{v} \to v_i$ at $\eta \to \infty$, is used. The boundary condition for v at the wall is $v = v_{w0}$ at $\eta = 0$. This condition leads to

$$\frac{i}{2\sigma}\left[A_1(1-G_0 r^2) - 2r\frac{\partial A_1}{\partial r}\right] + v_i = v_{w0}. \tag{4.15}$$

At the other boundary $\theta = \theta_1$ the coordinate should be stretched as $\theta_1 - \theta = E^{\frac{1}{2}}$. The equations corresponding to (4.9), (4.11), (4.13)–(4.15) are

$$\hat{u} = C_1(r)[e^{(-1-i)\sigma\eta} - e^{(-1+i)\sigma\eta}], \tag{4.16}$$

$$4ih^{\frac{1}{2}}C_1 - \frac{1}{G_0 r}\frac{\partial P_i}{\partial r} = T_{w1}(r), \tag{4.17}$$

$$\hat{T} = \tfrac{1}{2}(T_{w1} - T_i)[e^{(-1-i)\sigma\eta} + e^{(-1+i)\sigma\eta}] + T_i, \tag{4.18}$$

$$\hat{v} = \frac{1}{2\sigma}\left[(1+G_0 r^2)C_1 + r\frac{\partial C_1}{\partial r}\right][(-1+i)e^{(-1-i)\sigma\eta} - (-1-i)e^{(-1+i)\sigma\eta}]$$
$$+\tfrac{1}{2}C_1(3+G_0 r^2)\left[\left(\eta - \frac{-1+i}{2\sigma}\right)e^{(-1-i)\sigma\eta} - \left(\eta - \frac{-1-i}{2\sigma}\right)e^{(-1+i)\sigma\eta}\right] + v_i \tag{4.19}$$

$$-\frac{i}{2\sigma}\left[C_1(1-G_0 r^2) - 2r\frac{\partial C_1}{\partial r}\right] + v_i = v_{w1}. \tag{4.20}$$

5. Inner flow

In the inner core all variables do not depend on θ, therefore we can eliminate $\hat{P}_i$ by subtracting (4.17) from (4.11) to yield

$$X_a = A_1 - C_1 = \frac{T_{w0} - T_{w1}}{4ih^{\frac{1}{2}}}. \tag{5.1}$$

Eliminating v_i in a similar manner from (4.15) and (4.20), we have an equation for $X_s = A_1 + C_1$ as

$$\frac{dX_s}{dr} - \frac{1-G_0 r^2}{2r} X_s + \frac{\sigma}{ir}(v_{w0} - v_{w1}) = 0. \tag{5.2}$$

Integration of (5.2) yields

$$X_s = ih^{\frac{1}{4}} r^{\frac{1}{2}} \exp(-\tfrac{1}{4}G_0 r^2) \int_0^r \exp(\tfrac{1}{2}G_0 s^2)(v_{w0}(s) - v_{w1}(s))\, ds. \tag{5.3}$$

It is easy to derive

$$A_1 = \frac{T_{w0} - T_{w1}}{8ih^{\frac{1}{2}}} + \tfrac{1}{2}ih^{\frac{1}{4}} r^{\frac{1}{2}} \exp(-\tfrac{1}{4}G_0 r^2) \int_0^r \exp(\tfrac{1}{2}G_0 s^2)(v_{w0} - v_{w1})\, ds, \tag{5.4}$$

$$C_1 = -\frac{T_{w0} - T_{w1}}{8ih^{\frac{1}{2}}} + \tfrac{1}{2}ih^{\frac{1}{4}} r^{\frac{1}{2}} \exp(-\tfrac{1}{4}G_0 r^2) \int_0^r \exp(\tfrac{1}{2}G_0 s^2)(v_{w0} - v_{w1})\, ds. \tag{5.5}$$

By adding (4.15) and (4.20), we have an expression for v_i as

$$v_i(r) = -\frac{i}{2\sigma}\left[X_a(1 - G_0 r^2) - 2r\frac{dX_a}{dr}\right] + \tfrac{1}{2}(v_{w0} + v_{w1}). \tag{5.6}$$

The first term on the right-hand side of (5.6) represents an antisymmetric flow (see figure 3*b*), while the second term represents the symmetric one (see figure 4*b*). A thermally driven flow corresponds to the former, and a source/sink flow to the latter.

Other quantities in the inner core are easily obtained:

$$T_i(r) = \tfrac{1}{2}(T_{w0} + T_{w1}) - 2ih^{\frac{1}{2}} X_s, \tag{5.7}$$

$$\frac{\partial P_i}{\partial r} = -G_0 r T_i, \tag{5.8}$$

$$u_i(r) = -\frac{1}{4hr^2 \epsilon_R}\frac{d}{dr}(rT_i). \tag{5.9}$$

The first and second terms on the right-hand side of (5.7) are due to the antisymmetric and symmetric flows respectively. From (5.6) and (5.7) the statements given in §1 are easily derived.

6. The sidewall $E^{\frac{1}{3}}$ thermal layer

If there is no source/sink distribution at the sidewall $r = 1$ then X_s must be zero at $r = 1$ since the integrand in (5.3) represents a mass flux. Equation (5.7) implies that the inner temperature $T_i(r = 1)$ is the mean of $T_{w0}(1)$ and $T_{w1}(1)$. If the temperature of the sidewall has a distribution such that $T_{w2} = T_{w2}(\theta)$, then there must be a thermal boundary layer.

In the following we derive the boundary-layer equation (1.5), retaining z-dependence. Expecting the layer to be a $E^{\frac{1}{3}}$ layer, we can scale physical quantities as follows:

$$u = E^{\frac{1}{3}}\bar{u}, \quad v = \bar{v}, \quad w = \bar{w}, \quad P = E^{\frac{1}{3}}\bar{P}, \quad T = \bar{T}, \quad 1 - r = E^{\frac{1}{3}}\zeta. \tag{6.1}$$

Substituting (6.1) into the basic equations and retaining the lowest terms, we have

$$-\frac{\partial \bar{u}}{\partial \zeta} + \frac{\partial \bar{v}}{\partial \theta} + \frac{\partial \bar{w}}{\partial z} = 0, \tag{6.2}$$

$$-2\bar{v} + \bar{T} - \frac{1}{G_0}\frac{\partial \bar{P}}{\partial \zeta} = 0, \tag{6.3}$$

$$2\bar{u}+\frac{1}{G_0}\frac{\partial \bar{P}}{\partial \theta}=\frac{1}{\epsilon_R}\frac{\partial^2 \bar{v}}{\partial \zeta^2}, \tag{6.4}$$

$$\frac{1}{G_0}\frac{\partial \bar{P}}{\partial z}=\frac{1}{\epsilon_R}\frac{\partial^2 \bar{w}}{\partial \zeta^2}, \tag{6.5}$$

$$-4h\bar{u}=\frac{1}{\epsilon_R}\frac{\partial^2 \bar{T}}{\partial \zeta^2}. \tag{6.6}$$

A cross-differentiation of (6.3) and (6.4) eliminates $\bar{P}$ to give

$$\frac{\partial}{\partial \zeta}\left(\frac{1}{\epsilon_R}\frac{\partial^2 \bar{v}}{\partial \zeta^2}\right)-\frac{\partial \bar{T}}{\partial \theta}-2\frac{\partial \bar{w}}{\partial z}=0, \tag{6.7}$$

where (6.2) is used. By cross-differentiating (6.4) and (6.5) to eliminate $\bar{P}$, inserting (6.6) and integrating the resultant equation twice with respect to ζ, we have

$$\frac{\partial}{\partial z}(\bar{T}+2h\bar{v})-2h\frac{\partial \bar{w}}{\partial \theta}=0. \tag{6.8}$$

The continuity equation (6.2) can be written as

$$\frac{1}{4h}\frac{\partial}{\partial \zeta}\left(\frac{1}{\epsilon_R}\frac{\partial^2 \bar{T}}{\partial \zeta^2}\right)+\frac{\partial \bar{v}}{\partial \theta}+\frac{\partial \bar{w}}{\partial z}=0, \tag{6.9}$$

where (6.6) has been used.

Eliminating $\bar{v}$ and $\bar{w}$ in favour of $\bar{T}$ from (6.7)–(6.9), we obtain

$$\frac{\partial}{\partial \zeta}\left[\frac{1}{\epsilon_R}\frac{\partial^3}{\partial \zeta^3}\left(\frac{1}{\epsilon_R}\frac{\partial^2 \bar{T}}{\partial \zeta^2}\right)\right]+4(1+h)\frac{\partial^2 \bar{T}}{\partial z^2}+4h\frac{\partial^2 \bar{T}}{\partial \theta^2}=0. \tag{6.10}$$

If G_0 is $O(1)$, ϵ_R can be considered to be constant in the $E^{\frac{1}{3}}$ layer, and (6.10) reduces to (1.5).

The method of solution of (1.3) is essentially the same as that of (1.4), and is well known (see e.g. Matsuda 1977). Even if ϵ_R is retained, it is possible to solve the equation (Bark & Bark 1976; Durivault & Louvet 1976). In the present paper we do not repeat it.

The role of the $E^{\frac{1}{3}}$ thermal layer is twofold. First it mediates the temperature jump discussed above. As a result, a closed circulation whose flux is $O(E^{\frac{1}{3}})$ is generated, as is shown in figure 3 (*b*). Secondly fluid is rechannelled from the bottom buoyancy layer to the top one; the magnitude of the flux is $O(E^{\frac{1}{4}})$. These situations are also parallel to the case in the circular cylinder, and will not be discussed in detail.

The derivation of the governing equation of the $E^{\frac{1}{4}}$ thermal layer can be obtained in a similar manner to that above, and will not be discussed here.

7. Discussion

In the present paper a compressible counterpart of the Kuo–Veronis flow is investigated and new kinds of boundary layer are discovered. Kuo & Veronis (1971) pointed out that the topology of contours of geostrophic wind is important in deciding the nature of the flow. A geostrophic wind blows along an equal-depth line in the case of incompressible fluid with a free surface. If all the contours are closed, a geostrophic wind of order unity can blow. On the other hand, if none of the contours are closed, such as in the case of the pie-shaped basin, the flow is very weak and a

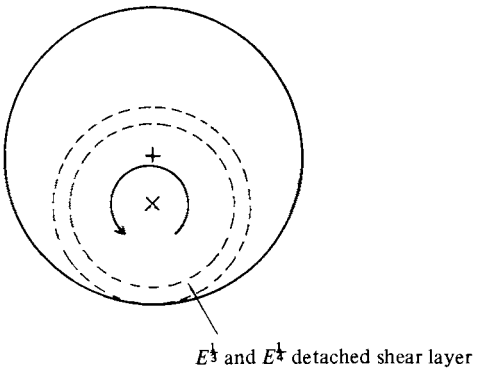

FIGURE 5. The (r, θ) cross-section of an off-axially rotating circular cylinder. The rotation axis is represented by $\times$, and the cylinder axis by $+$. The dotted circles show detached shear layers. Only within the inner dotted circle can a geostrophic and/or thermal wind of order unity blow.

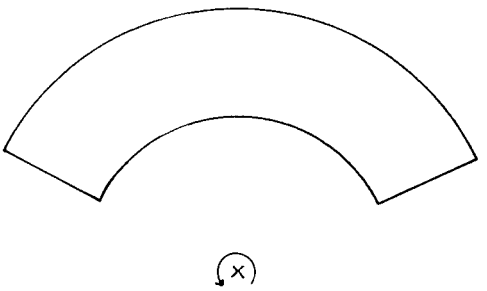

FIGURE 6. The (r, θ) cross-section of a truncated doughnut-shaped centrifuge.

phenomenon called westward intensification can be observed. Matsuda *et al.* (1981) investigated a gradual transition between the two extreme cases stated above.

Flows of compressible rotating fluid can also be understood in terms of the topology of the geostrophic contour. The geostrophic contour is nothing but a circle whose centre is the rotation axis in the compressible fluid. All geostrophic contours are closed in the circular cylinder considered in many papers, while none of them are closed in the pie-shaped cylinder.

It would be interesting to see an intermediate case. As an example let us consider a circular cylinder whose axis does not coincide with the rotation axis (see figure 5). A geostrophic wind (and a thermal wind as well) can blow only within the inner dotted circle, where all geostrophic contours are closed. In the region between the outer wall and the outer dotted circle is a dead-water region where only weak flow is possible. The dotted circles represent the $E^{\frac{1}{3}}$ and $E^{\frac{1}{4}}$ detached shear layers, whose character depends on the thermal boundary condition of the outer wall. A precise analysis of such flows is out of the scope of the present paper.

The present result may have some practical application. A conventional gas centrifuge for the enrichment of uranium is a rapidly rotating circular cylinder. If a counter-current is induced by the thermal, mechanical and/or external mechanism, the efficiency of the separation is generally proportional to the length of the cylinder and the fourth power of the peripheral speed. Considering these, we could construct

a truncated doughnut-shaped centrifuge or a conventional cylindrical centrifuge with radial walls in it. The counter-current is produced by the mechanism discussed above (see figure 6). The technical feasibility of such a centrifuge is, however, out of the scope of the present paper.

The authors wish to thank Prof. T. Sakurai for his comments, and a referee who suggested a unification of (1.3) and (1.4).

REFERENCES

BARCILON, V. & PEDLOSKY, J. 1967 Linear theory of rotating stratified fluid motions. *J. Fluid Mech.* **29**, 1–16.

BARK, F. H. & BARK, T. H. 1976 On vertical boundary layers in a rapidly rotating gas. *J. Fluid Mech.* **78**, 749–761.

DURIVAULT, J. & LOUVET, P. 1976 Etude de la couche de Stewartson compressible dans une centrifugense à contrecourant thermique. *C.R. Acad. Sci. Paris* **283**, 79–82.

KUO, H.-H. & VERONIS, G. 1971 The source–sink flow in a rotating system and its oceanic analogy. *J. Fluid Mech.* **45**, 441–464.

MATSUDA, T. 1977 On the importance of thermal boundary condition to the flow in a rapidly rotating gas. In *Proc. 2nd Workshop on Gases in Strong Rotation, Cadarache.*

MATSUDA, T., NAKAGAWA, K. & TAKEDA, H. 1981 Non-axisymmetric flow in a rotating cylinder. Incompressible and compressible fluid. In *Proc. 4th Workshop on Gases in Strong Rotation, Oxford.*

MATSUDA, T., SAKURAI, T. & TAKEDA, H. 1975 Source–sink flow in a gas centrifuge. *J. Fluid Mech.* **69**, 197–208.

MATSUDA, T. & TAKEDA, H. 1978 The structure of the Stewartson layers in a gas centrifuge. Part 2. *J. Fluid Mech.* **85**, 443–457.

NAKAYAMA, W. & USUI, S. 1974 Flow in rotating cylinder of gas centrifuge. *J. Nucl. Sci. Tech.* **11**, 242–262.

RÄTZ, E. 1978 Uranium isotope separation in the gas centrifuge. In *Lecture Series* 1978, *von Kármán Inst. for Fluid Dyn., Belgium.*

SAKURAI, T. & MATSUDA, T. 1974 Gasdynamics of a centrifugal machine. *J. Fluid Mech.* **62**, 727–736.

SOUBBARAMAYER 1979 Centrifugation. In *Uranium Enrichment* (ed. S. Villani), pp. 183–244. Springer.